JOURNAL OF AIRCRAFT
Vol. 41, No. 6, November–December 2004

Modeling Mechanical Fasteners in Single-Shear Lap Joints

Dale A. Cope* and Thomas E. Lacy†
Wichita State University, Wichita, Kansas 67260-0044

One central issue in damage tolerance analysis is the evaluation of stress intensity factors for cracks at fastener holes in mechanically fastened joints. Accurate solutions for stress intensity factors may be difficult to determine due to geometric complexity, along with variations in fastener load transfer and fastener interference. Detailed finite element models that include specific aspects of fastener geometry may be developed for lap joint analysis, but such representations are often impractical for large lap joints involving many fasteners. A methodology is derived that efficiently depicts mechanical fasteners in lap joints using finite elements. Fastener material properties are determined, based on an empirical force–displacement relationship, for highly refined fastener models, as well as for idealized spring element representations of fasteners. The two fastener characterizations are used in combination to develop computationally efficient models for determining loads, stresses, and stress intensity factors for cracks in lap joints. Parametric studies involving single-shear lap joints with three rows of fasteners indicate that both fastener representations provide comparable load transfer and relative displacement between mating sheets for a variety of fasteners. These studies also suggest that the particular fastener material has relatively little effect on stress intensity solutions, whereas the fastener diameter has a significant effect. Residual strength predictions are obtained for large bolted lap joints with multiple site damage, which are consistent with experimental results from the literature.

Introduction

THE evaluation of stress intensity factors (SIFs) for cracks in metallic joints is one of the central issues in a sound damage tolerance analysis. Accurate SIF solutions for cracks emanating from fastener holes may be difficult to determine for a given metallic joint with mechanical fasteners due to the structural complexity, along with variations in the fastener load transfer. Detailed finite element models of the structure and associated fasteners can be used to estimate the state of stress in a mechanically fastened joint. However, it is often impractical to model specific details explicitly of fastener geometry for structures containing a significant number of fasteners because explicit representation of fasteners often leads to numerical models with a prohibitively large number of degrees of freedom (DOF). To reduce the number of DOF in a particular model, individual fasteners connecting adjacent layered structures may be idealized using simple spring elements.[1] Predicated on St. Venant's principle, such representation may be appropriate in model regions sufficiently far removed from any crack tips of interest. Of course, the adopted spring force–displacement relationship has a substantial effect on the load transfer in a given joint, as well as on the SIF solutions for any cracks in the joint.[2] Commonly, various estimates of fastener flexibility are used to define a linear spring force–displacement relationship with an assumed equivalent spring constant.[2−4] Material properties for idealized spring element characterizations of fasteners must be selected carefully to ensure that the relative fastener displacement between sheets and the load transfer are approximately the same as for more refined representations that include explicit geometric details of the fastener, sheet materials, and their interface, that is, explicitly modeled fasteners.

In this study, elementary energy principles are used in combination with an empirical relation for fastener displacement to develop expressions for the effective elastic moduli of explicitly modeled mechanical fasteners and simplified linear spring fastener models. These fastener representations may be used in combination to provide an efficient means of modeling single shear lap joints with large numbers of mechanical fasteners. This study investigates the influence of various types of fasteners on the load transfer and SIFs in mechanically fastened lap joints. The influence of various fastener idealizations on calculated SIFs for cracks in for bolted lap joints with multiple site damage (MSD) is addressed. Numerically determined SIFs are used in two crack-tip linkup models to predict failure loads in bolted lap joints with MSD, and the calculated results are compared to experimental results from the literature.

Presented as Paper 2000-1368 at the AIAA 41st Structures, Structural Dynamics, and Materials Conference, Atlanta, GA, 3–6 April 2000; received 3 March 2002; revision received 15 March 2003; accepted for publication 14 July 2003.

*Research Scientist, National Institute for Aviation Research. Member AIAA.
†Assistant Professor, Department of Aerospace Engineering.

Modeling Fasteners in Lap Joints

Single-shear lap joints with three rows of mechanical fasteners are modeled using different combinations of explicit and spring element representations of fasteners to determine the appropriate level of model refinement necessary for accurate SIF solutions for cracks emanating from fastener holes. Special consideration was given to selection of spring constants for idealized spring fastener models that produced approximately the same load transfer and relative displacements between attaching sheets as explicitly modeled solid fasteners. The special purpose fracture analysis Code two-dimensional/layered (FRANC2D/L)[5,6] is used in this study to investigate various aspects of lap joint modeling. FRANC2D/L, which is available from http://www.mne.ksu.edu/∼franc2d/, is a highly interactive finite element program well suited to performing small deformation analyses of two-dimensional layered structures. The code allows for efficient SIF determination and incorporates an adaptive remeshing algorithm that facilitates mixed-mode crack propagation. The layered capability allows the user to model mechanically fastened and/or adhesively bonded structures, such as planar lap joints and bonded repairs. Individual structural components such as skins, stiffeners, and doublers may be modeled as separate layers in FRANC2D/L, each with its own associated finite element mesh. Overlapping layers may be defined with coincident midplanes or with an appropriate midplane offset to account for joint eccentricity. FRANC2D/L uses a linear bending algorithm to calculate automatically the bending stresses/strains and out-of-plane displacements in addition to the standard in-plane stress, strain, and displacement distributions.

As shown in Fig. 1, FRANC2D/L allows for both explicit and spring element representations of mechanical fasteners in layered structures. Explicit fastener models typically involve use of a combination of standard two-dimensional finite elements to define the

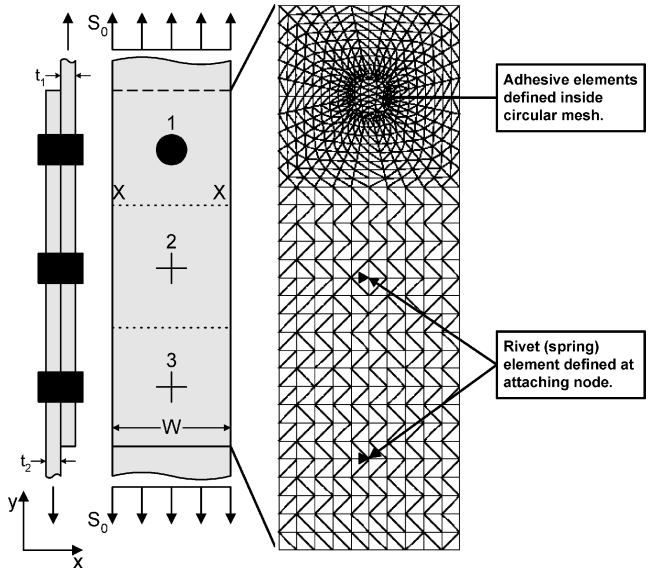

Fig. 1 Modeling fasteners in FRANC2D/L.

details of the fastener shank and sheet material in a given layer, nonlinear contact elements to define the interface between fastener and sheet (interface elements in FRANC2D/L), and adhesive elements to provide for distributed shear load transfer between overlapping fastener elements in adjacent layers. Simplified representations of mechanical fasteners connecting layered structures may also be obtained by defining spring elements (rivet elements in FRANC2D/L) that connect overlapping nodes in each layer. In this study, all explicit models of fasteners were assumed to be neat fit, that is, no interference, where fasteners were free to pull away from the sheet, but no interpenetration of fastener and sheet was allowed. Also, the interface between fastener and sheet was assumed to be frictionless, and the effect of joint clampup, that is, friction between mating sheets and increased fastener bending stiffness due to head and butt/collar bearing against mating sheets, was not considered.

Material properties for the adhesive elements, for example, shear modulus, modulus of elasticity, and joint eccentricity, and for the spring-rivet elements, for example, shear and bending stiffness, were selected to provide reasonable estimates of the relative fastener displacements and load transfer between the layers. These properties are defined based on appropriate measures of fastener flexibility, which may include both the effects of shear deformation and bending. Because fastener displacements may comprise more than 75% of the displacement in a joint,[2] it is essential that appropriate spring force–displacements are chosen to ensure displacement compatibility between the layers of sheet material. Errors up to 50% in crack-tip SIFs can result by neglecting fastener displacements.[2]

When the material properties of the adhesive elements between fastener layers are determined in FRANC2D/L, it is assumed that the fastener displacement is due to combined shear and bending loads. When linearly elastic material behavior is assumed, and the strain energy due to shear and bending is considered, the fastener displacement δ can be expressed as[7]

$$\delta = \frac{2 \cdot (1 + \nu) \cdot F \cdot h}{E_F \cdot A} + \frac{F \cdot h^3}{3 \cdot E_F \cdot I} \tag{1}$$

where ν is Poisson's ratio, F is the applied joint load, h is the joint eccentricity, A is the fastener cross-sectional area, I is the fastener moment of inertia, and E_F is the fastener elasticity modulus.

Through laboratory tests, Swift determined that fastener displacement could be represented by the following empirical relation[2]:

$$\delta = [F/(E \cdot d)][B + C \cdot (d/t_1 + d/t_2)] \tag{2}$$

where E is the sheet material elasticity modulus, d is the fastener diameter, t_1 and t_2 are the thicknesses of joined sheets, and B and C are nondimensional empirical constants. ($B = 5.0$ for aluminum fasteners, 4.0 for titanium fasteners, and 5/3 for steel fasteners, and $C = 0.8$ for aluminum fasteners, 0.82 for titanium fasteners, and 0.86 for steel fasteners.)

The fastener displacement using strain energy relations for shear and bending [Eq. (1)] may be equated to the empirical relation for fastener displacement (2) to develop the following relationships for the effective elasticity modulus E_F and shear modulus G_F of the fastener adhesive elements in FRANC2D/L:

$$E_F = (8 \cdot E \cdot h)/(\pi \cdot d)[(1 + \nu) + (8/3) \cdot (h/d)^2] \cdot [B + C \cdot (d/t_1 + d/t_2)]^{-1} \tag{3}$$

$$G_F = E_F/2 \cdot (1 + \nu) \tag{4}$$

Here the fastener cross-sectional area and moment of inertia are expressed in terms of the fastener diameter. These expressions provide relative compatibility of displacement between the mating sheets. Equations (3) and (4) may also be used to define the equivalent spring shear stiffness k_s and spring bending stiffness k_b associated with idealized spring-rivet representations of mechanical fasteners, that is,

$$k_s = \pi \cdot d^2 \cdot G_F/4 \cdot h \tag{5}$$

$$k_b = 3 \cdot \pi \cdot d^4 \cdot E_F/64 \cdot h^3 \tag{6}$$

When modeling mechanically fastened single-shear lap joints using a combination of explicit and simplified spring representations of fasteners, use of Eqs. (3–6) to define the fastener properties ensures that the simplified spring elements will provide approximately the same load transfer and relative displacement between sheets as explicitly modeled fasteners.

Fastener Stiffness Verification

It may be desirable to use explicitly modeled fasteners in combination with simplified spring-rivet elements to model fasteners efficiently in lap joints with large numbers of fasteners. To verify the feasibility of this approach, different combinations of explicitly modeled fasteners and spring-rivet fasteners were considered in single-shear lap joint models with three rows of fasteners (Figure 2, three such models).[8] In all three models, each layer consisted of 1.0-in. wide by 0.063-in. thick aluminum sheet material connected by three rows of 3/16-in.-diam aluminum fasteners. A remote tensile stress, $S_0 = 10{,}000$ psi, was applied to each model. Note that models C and D contain roughly 52 and 76%, respectively, of the DOF for model A. For this lap joint configuration, the explicit fastener adhesive properties were $E_F = 1.501 \times 10^6$ psi and $G_F = 5.643 \times 10^5$ psi, and the spring fastener stiffness properties were $k_s = 2.473 \times 10^5$ lb/in. and $k_b = 1.093 \times 10^6$ lb/in. For the explicit fasteners, a bilinear contact element was used to define the interface between the fastener and sheet, which assumed that the interface was infinitely stiff in compression and had no stiffness in tension. This bilinear contact element allowed the fastener to pull away from the sheet in tension, but it did not allow interpenetration of the fastener and sheet in compression.

Figure 3 shows a summary of the relative fastener centerline displacement and fastener load for the joint's upper fastener in all three models. These analysis results show that the calculated fastener displacements and loads of the upper fastener for either combination fastener model (model C or D) were within 1% of those where all fasteners are modeled explicitly (model A).[8] Comparable results were also found when considering the other two fasteners in the joint. These results suggest that combinations of explicit and spring element representations of fasteners may be used to develop computationally efficient lap joint models while retaining the essential features of the fastener displacement and load transfer within the joint.

The preceding results demonstrate that the spring force–displacement relationships for the spring-rivet element provide similar average displacement and load transfer characteristics as the explicitly modeled fasteners. This suggests that large lap joint models

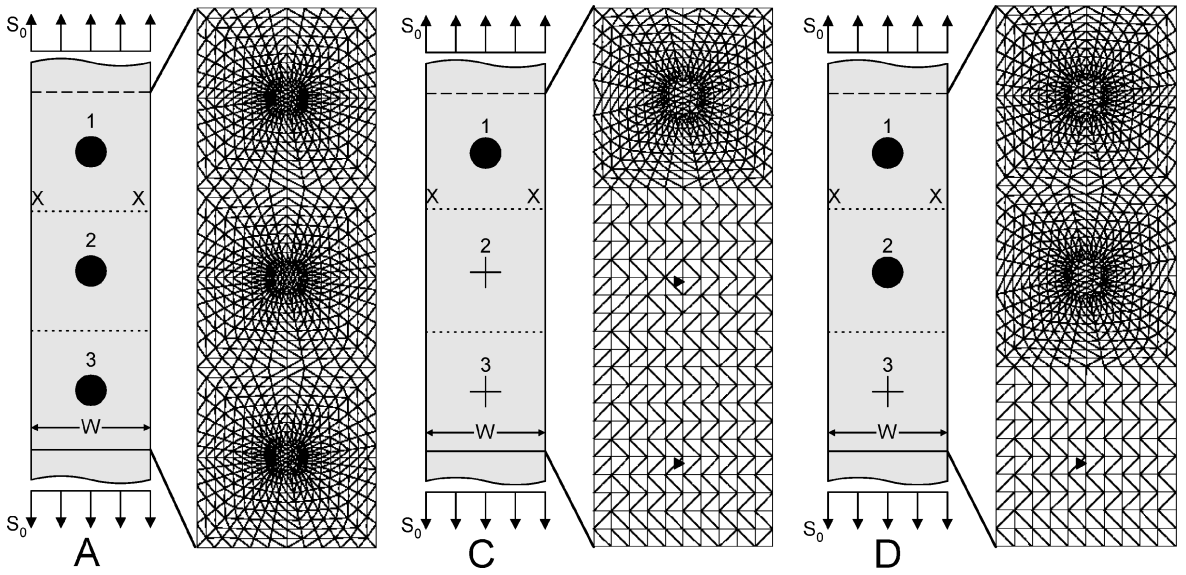

Fig. 2 Lap joint models with various fastener model combinations: model A, 3 explict fasteners; model C 1 explicit fastener; and model D, 2 explicit fasteners.

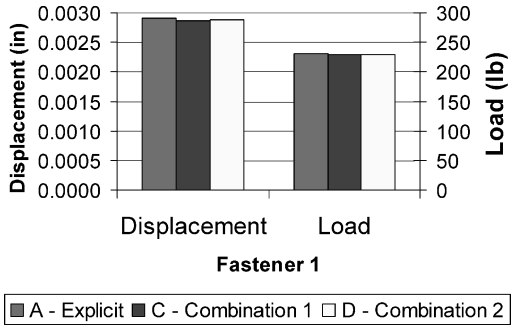

Fig. 3 Fastener displacements and loads for FRANC2D/L Models A, C, and D.

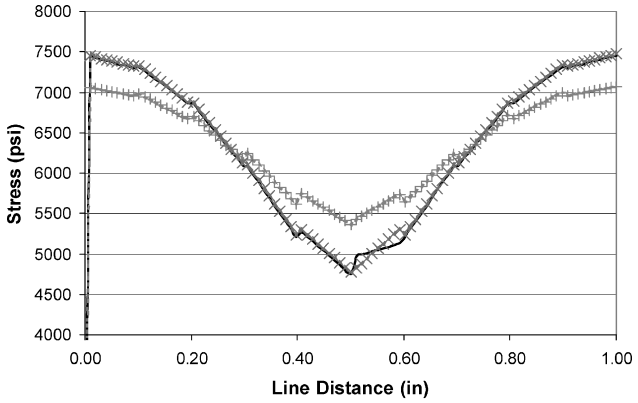

Fig. 4 Bypass stress distributions for FRANC2D/L models: ——, model A explicit; +, model C combination 1; and ×, model D-combination 2.

may be constructed using both explicit and spring element representations of mechanical fasteners without a significant loss of accuracy. Such a modeling technique may be used to substantially reduce the number of DOF in a given model. Of course, special care must be taken when introducing spring representations of fasteners in the vicinity of crack tips or in other model regions where accurate determination of local stress fields is paramount. The concentrated fastener load associated with the spring-rivet elements will result in a difference in the bypass stress distribution predicted by the two models. To illustrate this point, the calculated bypass stress distribution in the upper sheet of material for each of the three models is shown in Fig. 4. (Ref. 8). This stress distribution was taken along a horizontal line (X–X in Figs. 1 and 2) equidistant between the top two rows of fasteners calculated using models A, C, and D. The bypass stress distribution for the more refined combination fastener model (model D) is essentially the same as for the case where all fasteners are modeled explicitly (model A), whereas the bypass stress distribution for the less refined combination fastener model (model C) deviates somewhat from these two predictions. The difference in bypass stress distribution between models A and C is likely due to the higher stress concentration created by the spring element for the middle fastener in model C. For all three models, the mean bypass stress is essentially the same.

The purpose of incorporating explicit representations of fasteners in lap joint models is to achieve an accurate depiction of the local stress field in areas of interest, such as in the vicinity of cracks emanating from fastener holes. To illustrate this point, a radial crack was introduced at the critical upper fastener in the preceding models A, C, and D, as shown schematically in Fig. 5. For the given loading,

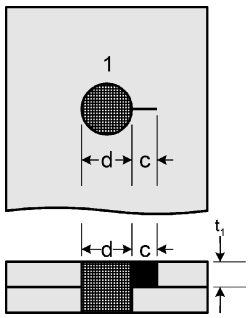

Fig. 5 Crack configuration at critical upper fastener.

mode 1 SIFs were calculated for crack lengths c, ranging from 0.04 to 0.26-in. expressed as nondimensionalized geometry (beta) factors, that is, $\beta = K/S_0 \cdot \pi c)^{1/2}$. Table 1 summarizes the results of the parametric study. Geometry factors calculated using the two models incorporating both explicit and spring element representations of fasteners (models C and D) were within 1.3% of those obtained using the more refined fastener model (model A).

A primary concern when analyzing lap joints is that joint eccentricity may result in significant bending stresses and/or out-of-plane displacements. Although FRANC2D/L has a linear bending algorithm that may be used to estimate bending stresses, strains, and out-of-plane displacements associated with joint eccentricity, SIF

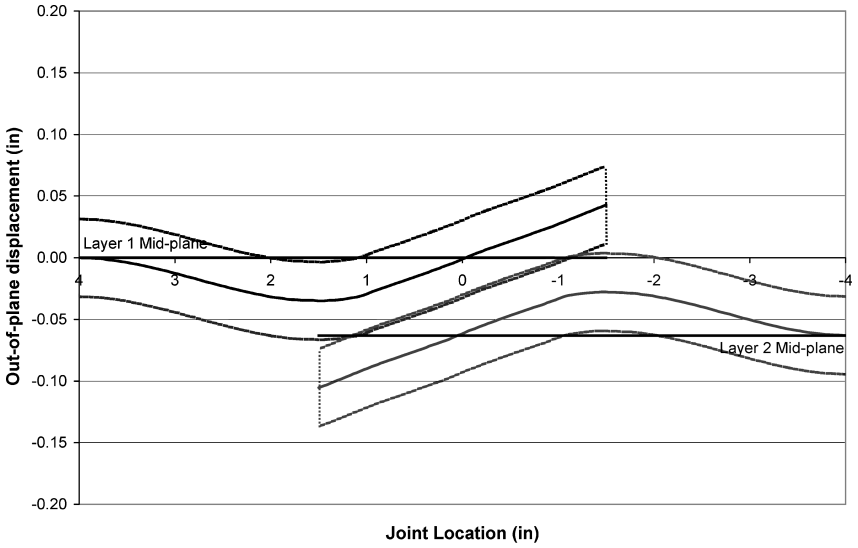

Fig. 6 Out-of-plane displacement in FRANC2D/L models A, C, and D: ——, layer 1, midplane displacements and ——, layer 2 midplane displacements.

Table 1 Geometry factor solutions for FRANC2D/L models A, C, and D

c/d	Model A explicit	Model C combination 1	Model D combination 2
0.213	2.147	2.153	2.174
0.320	1.803	1.787	1.801
0.427	1.563	1.562	1.558
0.533	1.426	1.422	1.425
0.640	1.323	1.322	1.322
0.747	1.238	1.231	1.237
0.853	1.188	1.184	1.189
0.960	1.143	1.139	1.143
1.067	1.105	1.100	1.105
1.173	1.079	1.075	1.079
1.280	1.037	1.063	1.049
1.387	1.064	1.060	1.064

solutions are based on the midplane stresses in a given layer. Figure 6 shows a typical out-of-plane displacement profile for models A, C, and D. Note that the peak out-of-plane displacement is roughly two-thirds of the plate thickness for the given analysis. Note that linear two-dimensional finite element analysis of bolted lap joints may be ill suited for the case where the out-of-plane displacements become large relative to the sheet thickness. A geometric nonlinear analysis may be necessary to account for the influence of bending effects appropriately due to joint eccentricity on the load transfer and calculated peak SIFs.

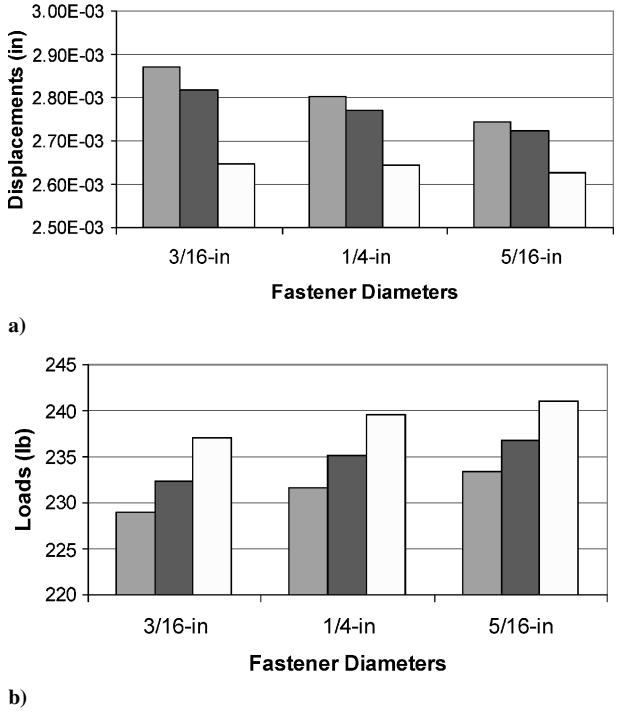

Fig. 7 Effect of various fasteners on upper fastener displacement and load: ■, aluminum; ■, titanium; and □, steel.

Analysis Studies

Lap Joints with Various Fastener Materials and Diameters

Parametric studies were performed to investigate the effect of fastener material properties and diameters on the relative displacement and load transfer in lap joints, as well as on the calculated SIFs for cracks emanating from fastener holes in the joints. Three fastener material types (aluminum, titanium, and steel) and three fastener diameters (3/16, 1/4, and 5/16 in.) were considered. The idealized lap joint model C, involving one explicit and two spring element fastener representations, was used in these evaluations, and the fastener material properties were calculated using Eqs. (3–6). Table 2 summarizes the calculated adhesive layer and spring element properties used in the FRANC2D/L analysis performed in this study. Note that some of the fastener diameters considered in this parametric study are somewhat large in comparison to the sheet thickness considered here; the data associated with such fasteners are included for reference purposes only to investigate the effect of fastener diameter.

When a lap joint geometry of 0.063-in. thick aluminum sheet material connected by three rows of fasteners with a remote tensile stress of 10,000 psi is used, Figs. 7a and 7b show the predicted relative upper fastener centerline displacement and fastener load, respectively, for each of the three fastener materials. For a given fastener diameter, use of steel fasteners tended to minimize the relative displacement of the upper fastener in the joint while maximizing the fastener load. Not surprisingly, the relative fastener displacements decreased with increasing fastener diameter, whereas the fastener load increased with increasing fastener diameter for the three materials.

Radial cracks were introduced at the critical upper fastener, that is, the lone explicitly modeled fastener, in each of the models used

Table 2 FRANC2D/L material properties for various fasteners

Fastener type	Elasticity modulus E_F, psi	Shear modulus G_F, psi	Shear stiffness k_s, lb/in.	Bending stiffness k_b, lb/in.
3/16-in. Aluminum	1.501E6	5.643E5	2.473E5	1.093E6
3/16-in. Titanium	1.650E6	6.203E5	2.719E5	1.201E6
3/16-in. Steel	2.159E6	8.118E5	3.558E6	1.572E6
1/4-in. Aluminum	8.902E5	3.346E5	2.607E5	2.048E6
1/4-in. Titanium	9.614E5	3.614E5	2.816E5	2.212E6
1/4-in. Steel	1.190E6	4.472E5	3.485E5	2.737E6
5/16-in. Aluminum	5.993E5	2.253E5	2.743E5	3.366E6
5/16-in. Titanium	6.389E5	2.402E5	2.924E5	3.589E6
5/16-in. Steel	7.603E5	2.858E5	3.480E5	4.270E6

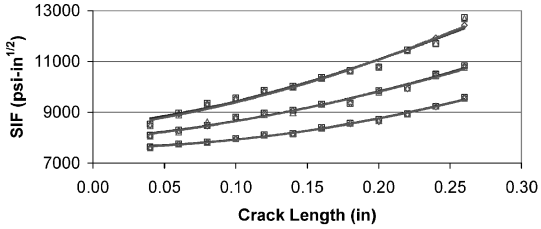

Fig. 8 Effect of various fasteners on stress intensity factors: □, aluminum; ◇, titanium; △, steel; ——, 3/16 in; - - - -, 1/4 in.; and – – –, 5/16 in.

in the fastener material study (Fig. 5). Figure 8 shows a summary of the results of SIF calculations performed for crack lengths ranging from 0.04 to 0.26 in. For a given fastener diameter, the calculated SIFs appear to be relatively insensitive to variations in fastener material properties over the range of crack lengths considered, even though the upper fastener load is somewhat dependent on the material properties of the fasteners for the uncracked case (Fig. 7b). The insensitivity of the SIFs to fastener material properties is likely because the load will be redistributed around the fastener hole when a crack is introduced, thereby reducing the load transfer across the upper fastener and decreasing its impact on SIFs. Increasing the fastener diameter tends to increase the respective calculated SIF by approximately 10% for a given crack length.

Bolted Lap Joint with Multiple Site Damage

Smith et al.[9] conducted an experimental investigation of the residual strength and critical linkup stress associated with a bolted lap joint containing lead cracks and MSD. With use of a combination of explicitly modeled fasteners and spring element representations of fasteners, FRANC2D/L was used to perform linear bending analyses of this bolted lap joint with a large crack and MSD cracks subjected to a remote tensile load, $S_0 = 10{,}000$ psi. Shown schematically in Fig. 9, the joint was constructed of two 24-in. wide 2024-T3 aluminum panels ($t_1 = t_2 = 0.056$ in.) fastened together with steel bolts ($d = 0.1875$ in). The bolt pitch, row spacing, and edge distance were 1, 1, and 1/2 in, respectively. To form the lead crack, slots of 8, 10, or 12 in. were introduced across the center fasteners in the upper row, and a lead crack tip was introduced at each of the outer two fasteners of the slot (Fig. 9) with an electromagnetic discharge machine (EDM) notch. MSD cracks were introduced with an EDM notch at the fasteners adjacent to the lead crack tips.

Figure 10 shows a portion of the finite element mesh used in the FRANC2D/L analysis for the bolted lap joint, illustrating how the three rows of fasteners are modeled. Each fastener in the upper row was modeled explicitly; no fastener interference was assumed. The fasteners in the remaining two rows were idealized using spring-rivet elements. SIFs were calculated for 27 different combinations of slot lengths (8, 10, and 12 in.), lead crack tip lengths (0.10, 0.15, and 0.20 in.), and MSD crack lengths (0.05, 0.10, 0.15, and 0.20 in.). Table 3 summarizes the calculated lead crack tip and worst-case MSD crack tip SIFs for all crack configurations considered in the study.

Table 3 Crack configurations and SIF solutions for bolted lap joint

Case	Slot length, in.	Lead crack length, in.	MSD crack length, in.	Lead crack SIF, psi · in.$^{1/2}$	MSD crack SIF psi · in.$^{1/2}$
1	8	0.10	0.05	4.007E+04	1.669E+04
2	8	0.10	0.10	4.053E+04	1.874E+04
3	8	0.15	0.05	3.978E+04	1.720E+04
4	8	0.15	0.10	4.028E+04	1.939E+04
5	8	0.15	0.15	4.091E+04	2.125E+04
6	8	0.20	0.05	3.971E+04	1.775E+04
7	8	0.20	0.10	4.028E+04	2.011E+04
8	8	0.20	0.15	4.100E+04	2.212E+04
9	8	0.20	0.20	4.189E+04	2.427E+04
10	10	0.10	0.05	4.662E+04	1.896E+04
11	10	0.10	0.10	4.715E+04	2.125E+04
12	10	0.15	0.05	4.628E+04	1.948E+04
13	10	0.15	0.10	4.686E+04	2.204E+04
14	10	0.15	0.15	4.758E+04	2.415E+04
15	10	0.20	0.05	4.618E+04	2.022E+04
16	10	0.20	0.10	4.683E+04	2.286E+04
17	10	0.20	0.15	4.766E+04	2.520E+04
18	10	0.20	0.20	4.869E+04	2.753E+04
19	12	0.10	0.05	5.353E+04	2.161E+04
20	12	0.10	0.10	5.414E+04	2.409E+04
21	12	0.15	0.05	5.351E+04	2.233E+04
22	12	0.15	0.10	5.419E+04	2.496E+04
23	12	0.15	0.15	5.504E+04	2.752E+04
24	12	0.20	0.05	5.310E+04	2.310E+04
25	12	0.20	0.10	5.385E+04	2.594E+04
26	12	0.20	0.15	5.481E+04	2.872E+04
27	12	0.20	0.20	5.600E+04	3.158E+04

The lead crack and MSD crack SIFs were used to compute nondimensionalized geometry factors (beta factors) for each of the considered crack configurations. Estimates of the remote failure load for each crack configuration were obtained using two linkup models, the Swift linkup model[10] and an empirically based modified linkup model developed by Smith et al.[11] The Swift linkup model presumes that failure will occur in a panel with MSD when the plastic zones of the lead and MSD cracks intersect (linkup) that is, when the ligament between the lead and MSD cracks reach net section yielding. The Swift link-up model[10] expresses the critical stress for ligament failure σ_{LU}, as:

$$\sigma_{LU} = \sigma_{ys} \cdot \sqrt{\frac{2 \cdot L}{a \cdot \beta_a^2 + l \cdot \beta_l^2}} \tag{7}$$

where σ_{ys} is the sheet material yield strength, L ligament length, that is, distance between lead and MSD crack tips, a the one-half lead crack length, β_a the lead crack geometry factor, l the one-half MSD crack length, and β_l the MSD crack geometry factor.

Because of significant differences between predicted and experimental failure stresses for flat 2024-T3 panels, Smith et al.[11] developed a modified linkup model that correlated reasonably well with experimental data. The Smith modified linkup model expresses

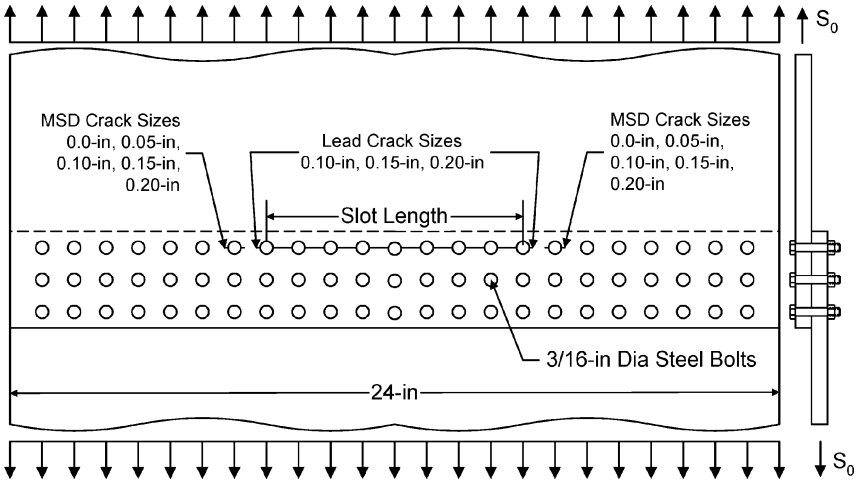

Fig. 9 Bolted lap joint.

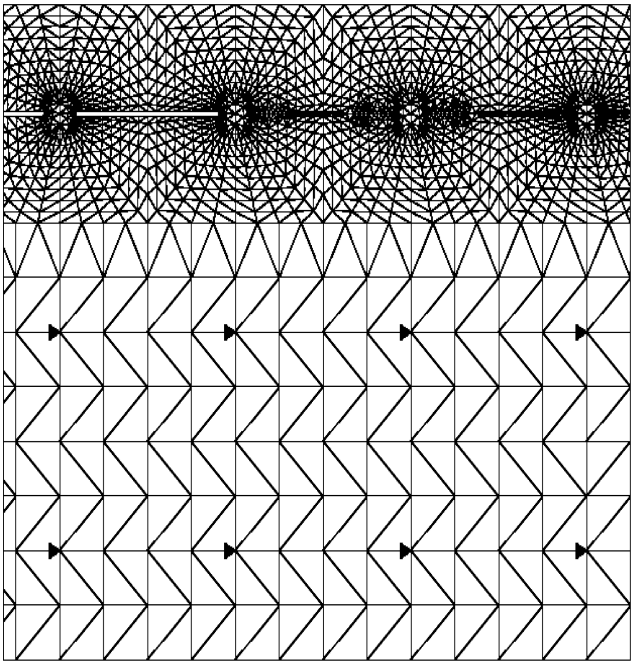

Fig. 10 Finite element mesh for bolted lap joint.

the critical linkup stress as

$$\sigma_C = \frac{\sigma_{\mathrm{LU}}}{C_3 \cdot \ell_n(a/L) + (C_4 + 1)} \tag{8}$$

The coefficients in Eq. (8) are $C_3 = -0.1806$ and $C_4 = 0.4791$, which were determined from an empirical analysis based on Military Handbook 5G (MIL-HDBK-5G) A-basis yield strength values of 40 ksi for clad 2024-T3 aluminum in the L-T direction. Table 4 summarizes the calculated geometry factors, predicted linkup (failure) stresses for both linkup models, and test failure stresses associated with each of the 27 combinations of lead crack lengths and MSD crack lengths.

Figure 11 shows a comparison of the predicted failure stresses obtained in this investigation to experimentally determined values obtained by Smith et al.[9] Using the Swift[10] linkup model, the difference between the predicted and experimental strength values ranged from 0.2 to 9.1% with an average error of 3.6%. For the Smith modified link-up model,[9] the differences ranges from 0.25 to 14.5% with an average error of 5.9%. Note that the Smith modified linkup model provides a more conservative estimate of the critical linkup stress than the Swift linkup model over the range of considered panels.

Table 4 Geometry factors and linkup stresses for bolted lap joint

Case	Lead crack β_a	MSD crack β_l	Swift linkup stress, ksi	Modified linkup stress, ksi	Test failure stress, ksi
1	1.1039	2.4836	18.801	16.408	18.378
2	1.1166	2.4020	17.573	15.529	16.786
3	1.0895	2.5595	18.106	16.030	18.378
4	1.1032	2.4853	16.821	15.098	16.443
5	1.1204	2.4284	15.570	14.189	15.454
6	1.0812	2.6413	17.288	15.547	17.374
7	1.0967	2.5776	15.943	14.557	16.473
8	1.1163	2.5278	14.637	13.594	15.342
9	1.1406	2.5264	13.302	12.596	14.725
10	1.1541	2.8214	16.216	14.645	15.565
11	1.1673	2.7237	15.173	13.881	14.881
12	1.1402	2.8987	15.628	14.320	15.365
13	1.1545	2.8250	14.522	13.497	14.107
14	1.1723	2.7598	13.452	12.701	13.095
15	1.1324	3.0089	14.917	13.886	14.821
16	1.1483	2.9301	13.774	13.026	13.958
17	1.1687	2.8797	12.648	12.175	12.798
18	1.1939	2.8658	11.513	11.307	11.882
19	1.2135	3.2157	14.137	13.146	12.954
20	1.2273	3.0877	13.242	12.478	12.515
21	1.2082	3.3228	13.533	12.770	12.738
22	1.2235	3.1993	12.604	12.068	11.786
23	1.2427	3.1449	11.664	11.351	10.878
24	1.1942	3.4374	12.986	12.451	12.247
25	1.2110	3.3249	12.009	11.703	11.577
26	1.2326	3.2820	11.020	10.936	10.751
27	1.2594	3.2874	10.016	10.149	10.037

In addition, for the cases with an 8- or 10-in. slot, the Swift linkup model generally matches the experimental data better than the Smith modified linkup model, as shown in Fig. 12. However, as the lead crack length increases from the nominal 10-in. slot to the 12-in. slot, the Smith modified linkup model more closely approximates the failure stress.

The large lap joint model developed in this study could have been simplified further by incorporation of spring element representations of fasteners at all fastener locations except those within several pitch diameters of the lead and MSD crack tips. Furthermore, the fasteners in the second row immediately below the lead and MSD crack tips could have been modeled explicitly to better to account for the variations in the bypass stress distributions predicted by the two fastener representations. In addition, an investigation into the influence of out-of-plane displacements and stiffening effects due to joint eccentricity on the calculated geometry factors is likely warranted. Nonetheless, the link-up model combined with linear elastic SIFs appeared to yield acceptable residual strength predictions for

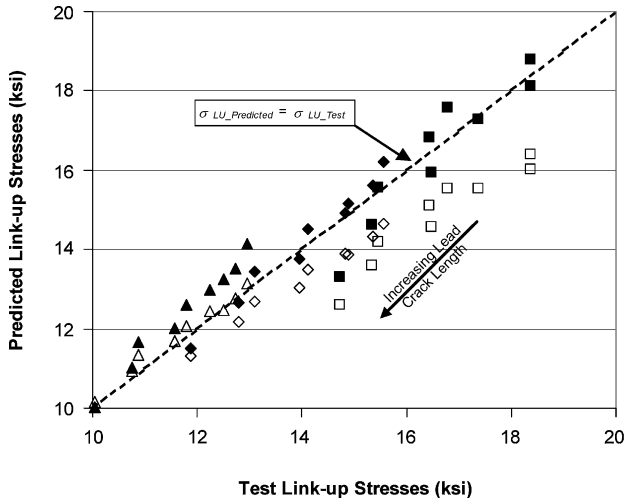

Fig. 11 Comparison of predicted linkup stresses to test linkup stresses: ■, 8-in. slot Swift linkup; □, 8-in. slot modified linkup; ♦, 10-in. slot Swift linkup; ◇, 10-in. slot modified linkup; ▲, 12-in. slot swift linkup; and △, 12-in. slot modified linkup.

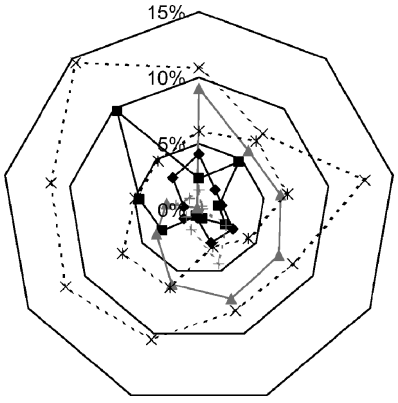

Fig. 12 Percentage error between predicted linkup stresses and test failure stress: ■, 8-in. slot swift linkup; ♦, 10-in. slot swift linkup; ▲, 12-in. slot swift linkup; ×, 8-in. slot modified linkup; ✳, 10-in. slot modified linkup; and +, 12.-in. slot modified linkup.

this case. These results suggest that combinations of explicit and spring element representations of fasteners may be used to develop computationally efficient lap joint models that provide reasonable estimates of the degradation in residual strength associated with MSD.

Summary

In the preceding discussion, limitations associated with modeling large mechanically fastened lap joints containing cracks were addressed. In particular, computational restrictions may prevent highly detailed finite element meshes that include explicit fastener representations. A methodology for efficiently depicting mechanical fasteners in lap joints using combined explicit and spring-rivet fastener models was implemented to facilitate numerical analysis of single-shear lap joints with MSD. The methodology used shear and bending stiffness equations that were derived to provide consistent element material properties between explicit and spring-rivet fastener models. Parametric studies involving single-shear lap joints with three rows of fasteners indicated that simplified fastener representations may be used to provide reasonable estimates of the load transfer and relative displacement between mating sheets for a variety of fastener diameters and materials. A bolted lap joint with a large lead crack and MSD was modeled using a combination of explicitly modeled fasteners and spring element representations of fasteners. SIF solutions were obtained for a range of lead crack and MSD crack lengths and used to perform residual strength calculations based on the Swift linkup equation and the Smith modified linkup equation. The residual strength predictions based on both theories compared favorably to experimental results from the literature.

These results suggest that combinations of explicit and spring element representations of fasteners may be used to develop computationally efficient lap joint models while retaining the essential features of the deformation and load transfer within the joint. Explicit representations of fasteners may be incorporated wherever an accurate depiction of the local stress field is required, such as in the vicinity of cracks emanating from fastener holes. Further investigations on the influence of geometric nonlinearity on the calculated results, as well as extension to three-dimensional problems, are likely warranted to develop fully the simplified fastener modeling approach implemented here. In addition, consideration of other issues such as fastener hole treatment, for example, fastener interference and cold working, and other joint configurations (butt joints, double-shear lap joints, etc.) may be desirable.

Acknowledgments

The authors are grateful to A. R. Ingraffea and P. Wawrzynek of Cornell University and M. A. James of NASA Langley Research Center for continued support of FRANC2D/L, as well as to B. L. Smith of Wichita State University for the use of experimental data for bolted lap joints.

References

[1]Dawicke, D. S., Phillips, E. P., Swenson, D. V., and Gondhalekar, S., "Crack Growth from Loaded Countersunk Rivet Holes," *Proceedings of the International Workshop on Structural Integrity of Aging Airplanes*, Atlanta Technology Publications, Atlanta, 1992, pp. 75–90.

[2]Swift, T., "Fracture Analysis of Stiffened Structure," *Damage Tolerance of Metallic Structures: Analysis Methods and Applications*, ASTM STP 842, edited by J. B. Chang and J. L. Rudd, American Society for Testing and Materials, West Conshohocken, PA, 1984, pp. 69–107.

[3]Huth, H., "Influence of Fastener Flexibility on the Prediction of Load Transfer and Fatigue Life for Multi-Row Joints," *Proceedings of the ASTM Symposium on Fatigue in Mechanically Fastened Composite and Metallic Joints*, ASTM STP 927, American Society for Testing and Materials, West Conshohocken, PA, 1985, pp. 221–250.

[4]Tate, M. B., and Rosenfeld, S. J., "Preliminary Investigation of the Loads Carried by Individual Bolts in Bolted Joints," NACA TN-1051, 1946.

[5]Dawicke, D. S., and Newman, J. C., Jr., "Analysis and Prediction of Multiple-Site Damage (MSD) Fatigue Crack Growth," NASA TP-3231, Aug. 1992.

[6]Wawrzynek, P., and Ingraffea, A. R., "Interactive Finite Element Analysis of Fracture Processes: An Integrated Approach," *Theoretical and Applied Fracture Mechanics*, Vol. 8, No. 2, 1987, pp. 137–150.

[7]Ugural, A. C., and Fenster, S. K., "Energy Method for Deflections," *Advanced Strength and Applied Elasticity*, 3rd ed., Prentice–Hall, Upper Saddle River, NJ, 1995, pp. 221–223.

[8]Cope, D. A., and Lacy, T. E., "Stress Intensity Determination in Lap Joints with Mechanical Fasteners," AIAA Paper 2000-1368, April 2000.

[9]Smith, B., Myose, R., and Lacy, T. E., "Multiple Site Damage in Aging Aircraft," Final Report for Advanced Design and Manufacturing Research Consortium, Aerospace Engineering Dept., Wichita State Univ., Wichita, KS, 1999.

[10]Swift, T., "Widespread Fatigue Damage Monitoring—Issues and Concerns," *FAA/NASA International Symposium on Advanced Structural Integrity Methods for Airframe Durability and Damage Tolerance*, NASA CP-3274, Pt. 2, 1994, pp. 829–870.

[11]Smith, B. L., Saville, P. A., Mouak, A., and Myose, R. Y., "Strength of 2024-T3 Aluminum Panels with Multiple Site Damage," *Journal of Aircraft*, Vol. 37, No. 2, 2000, pp. 325–331.